Quantifying Climate Change Risk through Natural Hazard Losses to Inform Adaptation Action

SUPPLEMENTARY INFORMATION

These supplemental materials detail the methods of parts of the analysis. The aim of these supplemental materials are to increase ability to recreate the analysis and provide additional technical details. These materials include information on hazard: details on coastal flooding and how sea level rise (SLR) is added to tsunami hazard, and on vulnerability: on the forms of the vulnerability functions used for earthquake, coastal flooding, and tsunami.

HAZARD METHODS

Coastal flooding

Coastal flooding hazard is adopted from the Adapting to Rising Tides maps (Vandever et al., 2017). These maps utilize the 'One Map, Many Futures' approach, which means that the same map may represent, for example, mean higher high water with 36 inches of SLR, 1-year storm surge with 24 inches of SLR, 2-year storm surge with 18 inches of SLR, 5-year storm surge with 12 inches of SLR, 25-year storm surge with six inches of SLR, and the present-day 50-year storm surge. This approach allows fewer total maps to be used to represent many future scenarios. By utilizing these maps, we reconstruct flood hazard curves for Alameda, filling in return periods that are missing for each level of SLR. Since Alameda is a relatively small study area, the flood hazard is all coming from the same mechanism, coastal storm surge, and the entire island is assumed to experience its maximum storm surge from the same event. We find that water depth versus return period (RP) is approximately log-linear, and use that interpolation to obtain water depth values at each location for each missing SLR-RP combination. As a lower bound on the flood risk, values below known flood depths are set to zero. This lower bound avoids overestimation of flood depths at frequent return periods and in present-day conditions where flood occurrence is rare. Since sea level rise amounts are given in imperial units, we approximate with the closest amount that is within three inches, or 7.62 cm, to the levels we use in the metric system. In the case where one higher amount and one lower amount or SLR exist each three inches away, we fill in hazard curves for both and take the average value between them. This is the case for 1 m, which is between 36 and 42 inches.

Tsunami

Tsunami hazard maps are provided for present-day conditions from the California Geological Survey (State of California, 2023). Since tsunami maps are not provided for future sea levels, we add SLR to the given maps. We assume linearity with sea level rise, so that for locations with tsunami hazard, the depth will increase by the amount of sea level rise. However, for locations that are beyond the edge of present-day inundation, we account for the land elevation in modeling future sea levels. New locations that may experience tsunami inundation but do not have tsunami risk at present-day are identified by the ratio of tsunami amplitude (amp) minus land elevation ($elev$) versus water depth (d). At present, the relationship between $amp - elev$ and water depth, d, is shown in Fig. S1. Those values that are greater than -2 at present day experience tsunami inundation, so those that have values greater than -2 when adding on SLR are considered to experience tsunami inundation in future sea level scenarios. This relationship is consistent across tsunami return periods, so it is assumed to apply to any future case under SLR.

In future climate scenarios, there are three categories to add SLR. These categories include combinations of location and return period. The first category experience tsunami in present-day. Those locations have a simple addition of the SLR amount (slr) to the present-day water depth, $d_{slr} = d_0 + slr$. The second category are not flooded in present-day, but have a value of $amp - elev < -2$. This inequality signifies that they are not expected to flood at present, but may in the future. This category has future water depth defined by

$$d_{slr} = \begin{cases} 0 & \text{if } amp - elev + slr < -2 \\ 0.95 \times (amp - elev + slr) + 1.78 & \text{if } amp - elev + slr \geq -2 \end{cases} \quad (1)$$

where slr is the amount of SLR for the given scenario, amp is the present-day tsunami amplitude, and $elev$ is the ground elevation at the location. This equation brings sites which are currently not flooded into the flood zone considering a larger tsunami amplitude. The third category is where we expect flooding at present-day, but there is none. These are locations where the $amp - elev \geq -2$, however $d_0 = 0$. This category is interpolated from known return periods at the same location. The form of interpolation is log-linear, to align with the pattern of known data. Generally, this is a fit between expected zero locations and known inundation at the highest return periods. With these three categories, all water depths are modeled for future SLR.

To apply the linear sea level rise assumption, amplitude is increased by 2 m uniformly, and the elevation remains the present-day land elevation. Eqn. 1 is applied to determine the inundation depth under future SLR scenarios.

VULNERABILITY METHODS

This section details the methods and vulnerability functions utilized for each hazard.

Earthquake

In general, vulnerability functions are taken directly from their sources. For earthquake, a combined vulnerability function is used to combine ground shaking and liquefaction loss. For ground shaking, the Hazus fragility functions are used, which depend

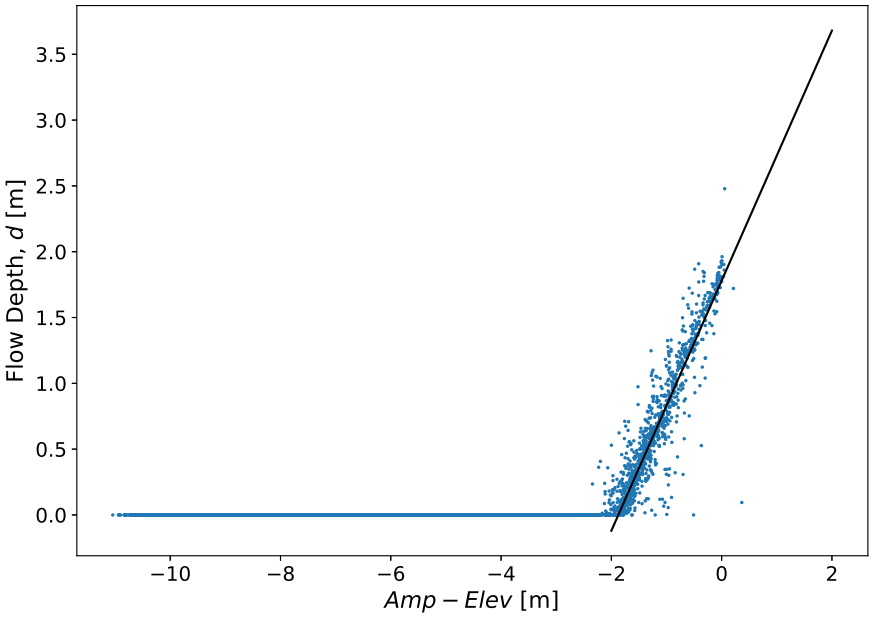

(a) 975-year return period

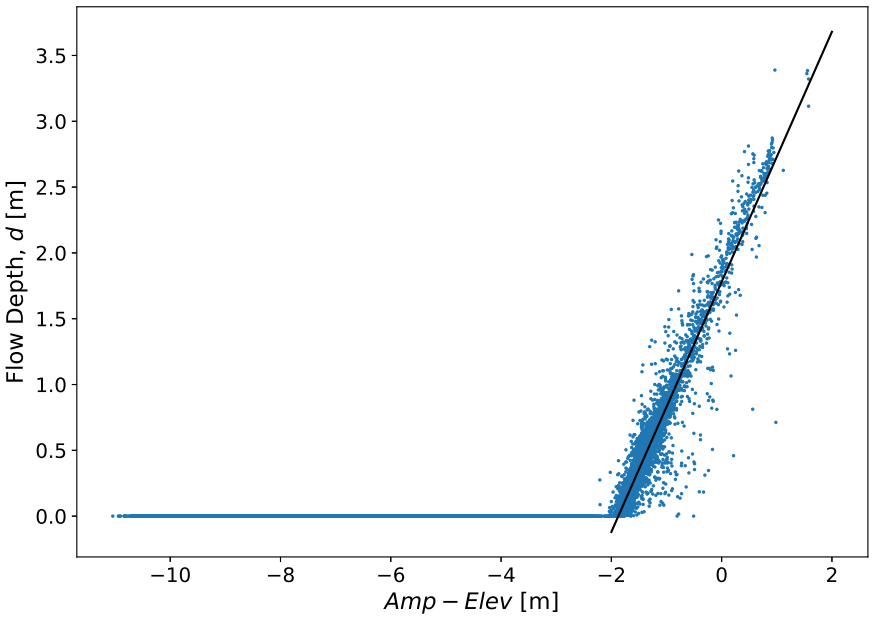

(b) 2475-year return period

Fig. S1. Inundation depth versus $amp - elev$ for the present-day tsunami at multiple return periods. Each point represents one location in the study area. The black trendline shows the assumed relationship for future climate scenarios, given by Eqn. 1.

on structural type and code level (Federal Emergency Management Agency (FEMA), 2003). These are assigned to the building stock based on their year of construction

and occupancy type (Federal Emergency Management Agency (FEMA), 2002). Loss ratio from ground shaking, LR_{gs}, is a summation of the loss ratio from structural, non-structural drift-sensitive, and nonstructural acceleration-sensitive component damages. Each of these components are a function of peak ground acceleration, pga. Thus, loss ratio from ground shaking can be described as

$$LR_{gs} = f_{code,str}(pga) \tag{2}$$

where $code$ represents the code level of construction, based on region of interest and defined by Hazus, str represents structural type, as defined in the Hazus framework (Federal Emergency Management Agency (FEMA), 2002), and pga is the peak ground acceleration at the site.

For liquefaction hazard, the vulnerability function from (Geyin et al., 2020) is approximated as

$$LR_{liq} = 0.117 \times LPI^{0.46} \tag{3}$$

where LR_{liq} is the loss ratio due to liquefaction as a function of liquefaction potential index, LPI. There is no distinction between code levels, construction years, number of stories, or structural types for the liquefaction vulnerability function. Thus, the function is applied to all buildings in the inventory. Since the function was fit on single-family residential structures, we only apply it to small residential structures under three stories, which are mostly wood frame construction consistent with the empirical training data (Geyin and Maurer, 2020).

Since the liquefaction vulnerability function represents all damage to a building, the final loss ratio for each building is taken as

$$LR_{eq} = max(LR_{gs}, LR_{liq}) \tag{4}$$

Thus, LR_{eq} is a function of pga and LPI. Since LR_{gs} includes damage from shaking alone and LR_{liq} combines shaking and liquefaction, in general, LR_{liq} will dominate in locations with liquefaction hazard.

Seismic retrofit adaptation

Since the seismic retrofit adaptation is focused on year of construction, it only affects the LR_{gs}. The seismic retrofit involves increasing the construction year to modern code-compliant buildings, or 'high code.' Since this would reduce the shaking damage that is wrapped into the LR_{liq}, we subtract the reduction in shaking loss from the liquefaction loss, and then take the maximum of the two. While it is hard to physically separate the source of damages in an earthquake, this represents the benefit that is expected from reduced shaking damage in the case where there is strong shaking and liquefaction.

Coastal flooding

The coastal flood vulnerability function is adopted from Wing et al. (2020). These functions are in the form of beta functions, defined for each depth of flooding from one foot to seven feet, excluding six feet. Values are interpolated for water depths between these discrete values, and skewed values are set for zero depth for cases where it is

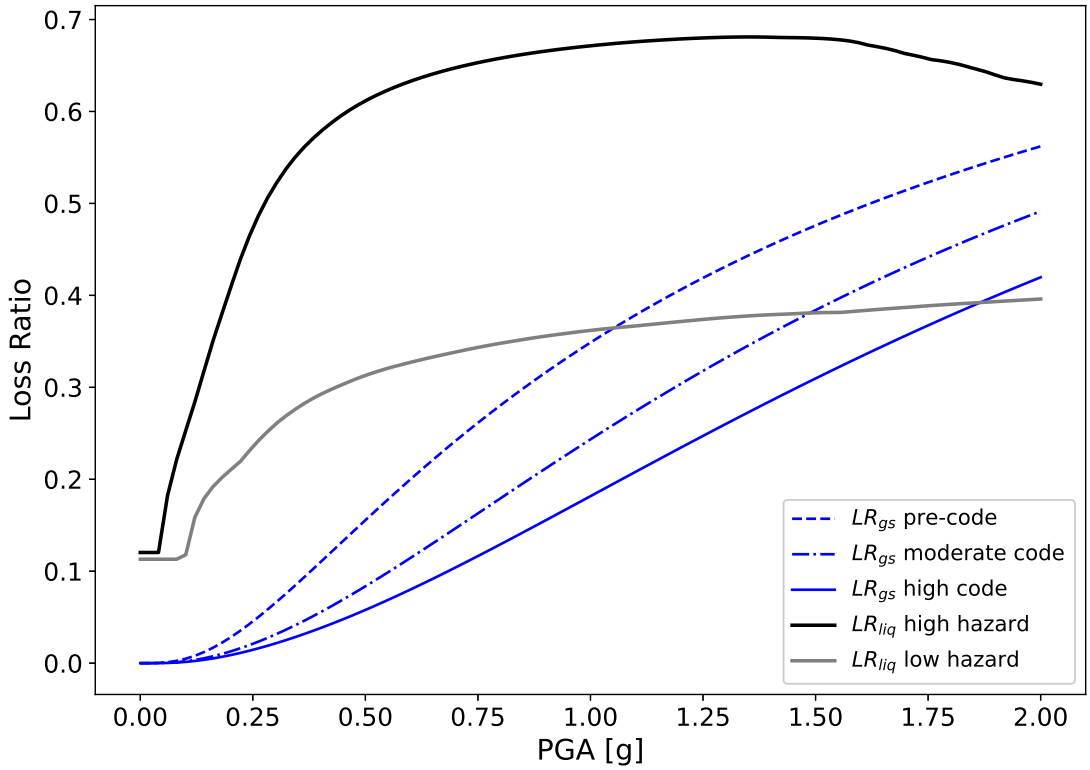

Fig. S2. Loss ratios due to ground shaking and liquefaction versus pga. For liquefaction losses, this assumes a M7.0 earthquake and is performed for example low and high liquefaction risk locations. For ground shaking losses, curves are shown for pre-, moderate, and high seismic code levels.

needed to interpolate between zero and one foot. The skewed values used are $\alpha = 0.01$ and $\beta = 10$. These values are not used for zero depth, which results in zero damage. For depths above seven feet, the seven foot parameters are utilized. Fig. S3 shows the expected value of loss ratio due to coastal flooding versus depth based on the beta value parameters.

Based on the San Francisco depth-damage curves from Hazus (Davis and Skaggs, 1992; Federal Emergency Management Agency (FEMA), 2021), loss ratios of two-story buildings to one-story buildings are approximately half. Thus, to avoid overestimation of damage to large, expensive multi-story buildings in Alameda, we assume that the loss ratio can be approximated by dividing the loss ratio by the number of stories. Even the deepest floods of eight to ten feet would only affect the first story of a building, so this is a reasonable approximation. Our case study only includes one- to three-story buildings; the curves for each of the numbers of stories are shown in Fig. S3.

Tsunami

The tsunami vulnerability functions are adapted from Suppasri et al. (2013). The functions are given for one, two, and three story buildings, which are the heights included in the Alameda exposure data. As given, the vulnerability functions map inundation

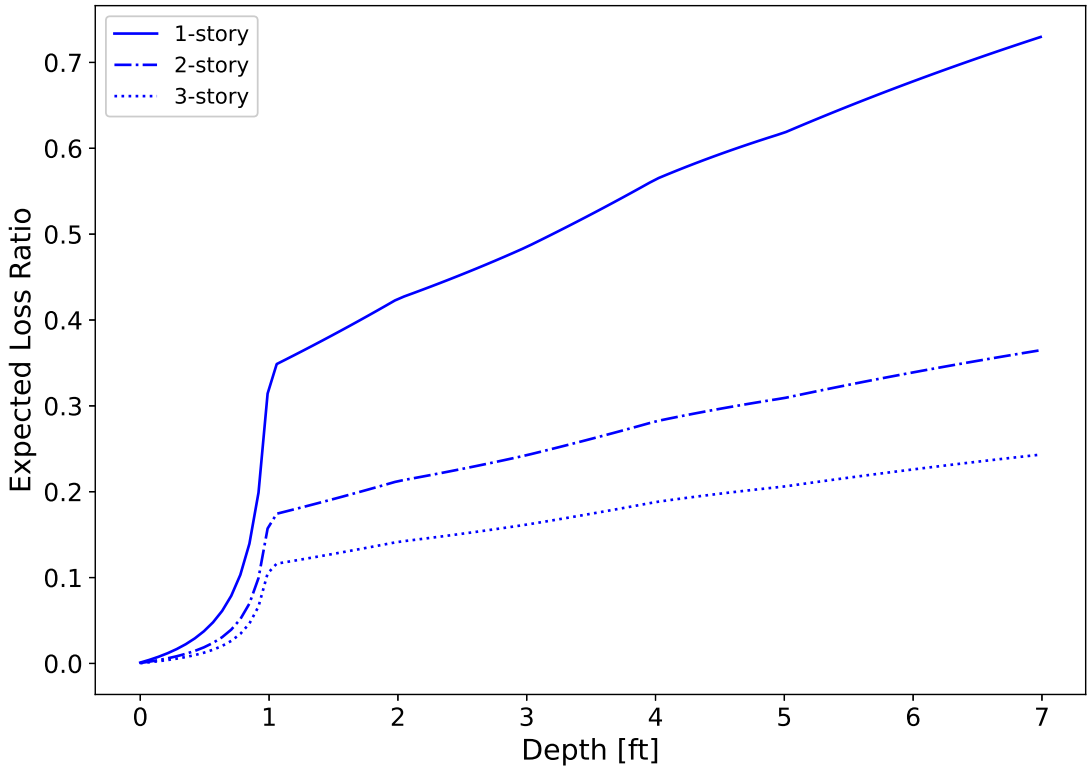

Fig. S3. Expected loss ratio from the beta fragility function versus water depth, d.

depth to probability of being in each of six damage states: minor, moderate, major, complete, collapse, and washed away. We combine collapse and washed away into one damage state. These are mapped to loss ratios from zero to one based on analogous damage states defined in Goda and De Risi (2017). The expected values based on 50000 samples are plotted in Fig. S4 for one, two, and three story buildings.

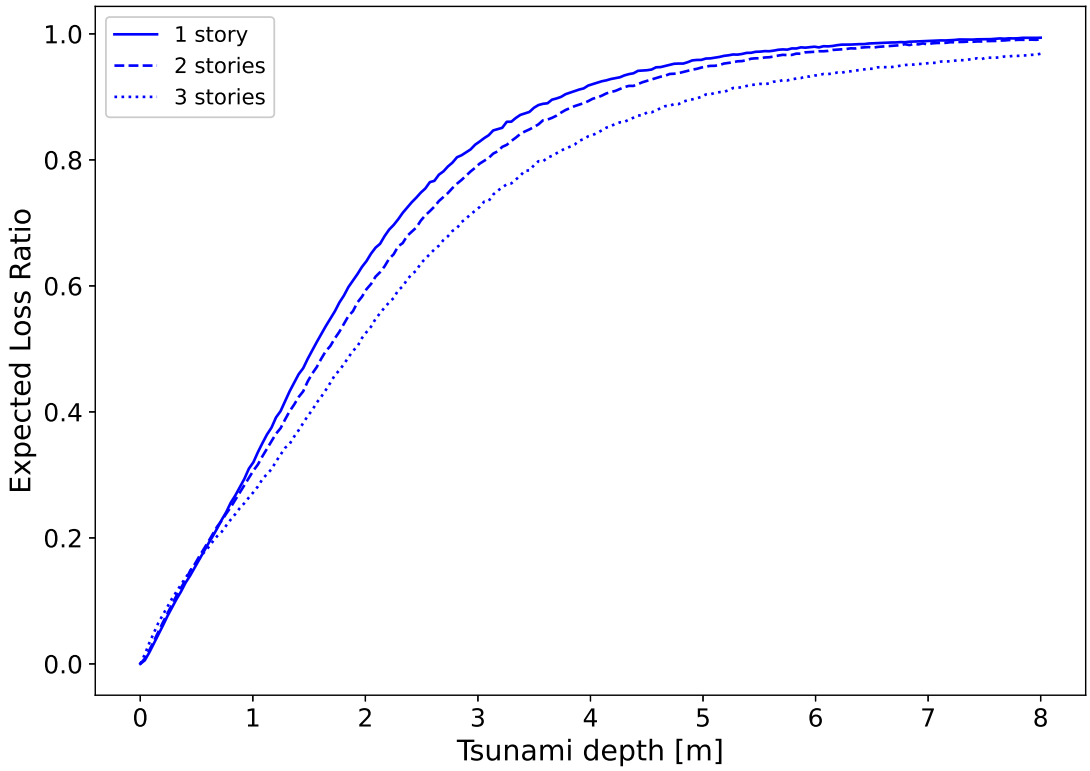

Fig. S4. Expected loss ratio versus inundation depth for tsunami based on number of stories.

REFERENCES

Davis, S. A. and Skaggs, L. L. (1992). "Catalog of residential depth-damage functions used by the army corps of engineers in flood damage estimation." *Report No. IWR Report 92-R-3*, U.S. Army Corps of Engineers, Institute for Water Resources, Ft. Belvoir, VA.

Federal Emergency Management Agency (FEMA) (2002). *Hazus-MH 2.1 Technical Manual*. Department of Homeland Security, Washington, D.C.

Federal Emergency Management Agency (FEMA) (2003). *HAZUS-MH MR4 Technical Manual*. Department of Homeland Security, Washington, D.C.

Federal Emergency Management Agency (FEMA) (2021). *Hazus Flood Model Technical Manual, Version 5.1*. Accessed: 2024-09-16.

Geyin, M. and Maurer, B. (2020). "Fragility functions for liquefaction-induced ground failure." *Journal of Geotechnical and Geoenvironmental Engineering*, 146(12), 04020142.

Geyin, M., Maurer, B., and van Ballegooy, S. (2020). "Lifecycle liquefaction hazard assessment and mitigation." *Geo-Congress 2020*, Reston, VA:American Society of Civil Engineers, 312–320.

Goda, K. and De Risi, R. (2017). "Probabilistic tsunami loss estimation methodology: stochastic earthquake scenario approach." *Earthquake spectra*, 33(4), 1301–1323.

State of California (2023). "Probabilistic Tsunami Hazard Analysis Raster Data – Version 1. California Geological Survey and AECOM Technical Services; dated 2023, accessed April 19, 2024.

Suppasri, A., Mas, E., Charvet, I., Gunasekera, R., Imai, K., Fukutani, Y., Abe, Y., and Imamura, F. (2013). "Building damage characteristics based on surveyed data and fragility curves of the 2011 great east japan tsunami." *Natural Hazards*, 66, 319–341.

Vandever, J., Lightner, M., Kassem, S., Guyenet, J., Mak, M., and Bonham-Carter, C. (2017). "Adapting to rising tides bay area sea level rise analysis and mapping project." *URL: http://www. adaptingtorisingtides. org/wp-content/uploads/2018/07/BATA-ART-SLR-Analysis-and-Mapping-Report-Final-20170908. pdf*.

Wing, O. E., Pinter, N., Bates, P. D., and Kousky, C. (2020). "New insights into us flood vulnerability revealed from flood insurance big data." *Nature communications*, 11(1), 1444.